

# On the azimuth angle characteristics of the blast wave from an underground magazine model (V) —Experiments on the effects of length ratio between magazine chambers and passageways—

Yuta Sugiyama<sup>\*†</sup>, Kunihiko Wakabayashi<sup>\*</sup>, Tomoharu Matsumura<sup>\*</sup>, and Yoshio Nakayama<sup>\*</sup>

<sup>\*</sup>National Institute of Advanced Industrial Science and Technology (AIST), Central 5, 1-1-1 Higashi, Tsukuba-shi, Ibaraki, 305-8565 JAPAN

Phone: +81-29-861-0552

<sup>†</sup>Corresponding author: yuta.sugiyama@aist.go.jp

Received: May 7, 2018 Accepted: September 20, 2018

## Abstract

In this article, we report small-scale explosion experiments for assessing the effect of the shape of an underground magazine model on blast-wave propagation outside the magazine. The underground magazine model was divided into chamber and passageway sections. The internal diameters of the chamber and passageway sections were 38.8 mm and 19.8 mm, respectively. The length ratio  $L_1/L_0$  between the chamber ( $L_0$ ) and passageway ( $L_1$ ) lengths varied from 0.125 to 2.0 in the experiments. The data was compared with previously reported experimental data from a model-scale magazine with a uniform inner diameter of 38.8 mm. Explosion experiments with this model provided the azimuthal distributions of peak overpressure and positive impulse caused by blast waves exiting the magazine. The interaction between the blast wave and the junction of the chamber and the passageway caused the multiple blast waves and multiple overpressure peaks appearing in pressure-time histories. A narrow passageway greatly mitigated the peak overpressure outside the magazine, but the ratio of the chamber to the passageway length showed no effect in the present conditions. The multiple blast waves tended to increase the positive impulse if the magazine was relatively narrow. The shape of isobars of the peak overpressure was independent of the length of the passageway in the present study.

**Keywords:** scale model experiment, azimuthal overpressure distribution, high-explosive magazine, hazardous materials management

## 1. Introduction

Accidental initiation of high explosive materials rapidly releases a large amount of energy, and this generates a blast wave. Incident shock waves cause a sudden increase in the local overpressure, followed by a subsonic flow and gradually decreasing overpressure. The blast parameters of peak overpressure and positive impulse allow the estimation of the physical hazard posed by an explosion. The peak overpressure is an instantaneous value, whereas the positive impulse is an integral that indicates the blast-wave strength. Generally, these two blast parameters are closely related, and the severity of damage caused depends on the distance between the magazine, where

explosives are stored, and an adjacent residential area<sup>1)</sup>. Appropriate standards for the storage of high explosive materials in magazines can be developed in terms of these measurements.

The so-called shotgun magazines, which are constructed underground, are regulated by the Explosive Control Act in Japan. The area within the explosives safety quantity distance (ESQD) should be secured uniformly from the outside wall of the underground magazine to nearby residential areas. The situation in which an explosive is detonated in an underground magazine exhibits blast-wave expansion like that from a shock tube, which affects the effective ESQD in front of the magazine entrance<sup>2),3)</sup>.

The generated blast wave exits the underground magazine via the entrance as a blast wave with maximum peak overpressure flowing along the exit direction. Then, any increment in the azimuth angle around the exit direction weakens the blast wave<sup>4)</sup>. ESQD values should be corrected for the azimuthal distribution of blast-wave strength around the magazine exit.

Since the peak-overpressure distribution at the ground is the most influential factor determining the ESQD, we performed a series of experiments with small-scale explosion experiments<sup>5),6)</sup>, numerical simulations<sup>7)</sup>, and field experiments<sup>8)</sup> to determine how the effective ESQD varies azimuthally around the magazine exit. In our previous work, the cross section of the underground magazine was assumed to be circular with a uniform inner diameter. The internal length-to-diameter ratio of the magazine,  $L/D$  was fixed to 3 in order to focus on the propagation behavior of the blast wave<sup>5),7),8)</sup>. We formulated an empirical equation for the peak-overpressure distribution, which accurately estimated the azimuthal distribution of blast-wave strength once the blast wave was fully developed outside of a magazine opening<sup>5)</sup>.

Underground magazines with different shapes have different values of  $L/D$  and loading density, which is the ratio of the mass of stored explosive to the volume of the magazine chamber<sup>9)-11)</sup>. In order to estimate the peak-overpressure distribution in case of an arbitrarily shaped underground magazine, we need to model how the magazine shape affects the blast-wave propagation. The one-dimensional shock-tube theory predicts that shock waves weaken by an expansion wave from the end wall. Therefore, a long tube may attenuate both the shock wave inside and the blast wave outside the underground magazine, effectively shortening the ESQD. As a first step to discuss the effect of magazine shape, we experimentally tested the effect of  $L/D$  using underground magazines with  $L/D = 9$  and  $21$ <sup>6)</sup>. With the higher  $L/D$  tested in this experiment, the peak overpressures of the blast wave outside the magazine were relatively lower. This result suggests that the ESQD around a magazine is affected by  $L/D$  of an underground magazine.

Previously, we only considered underground magazines shaped like a simple tube, in which the cross-sectional area was constant over the whole length of the magazine. However, the underground magazine might be divided into a chamber for storing the explosive material and a passageway for carrying material from the magazine entrance to and from the chamber. The passageway is generally narrower than the chamber. Previous researches<sup>2),12)</sup> indicated that the size of the tube exit determines the strength of the blast wave outside the magazine. We expected that decreasing the size of the exit should mitigate the blast-wave strength outside the underground magazine, so that the ESQD may be functionally related to the difference in the cross-sectional areas of the two sections. Therefore, as a next step in estimating the peak-overpressure distribution outside an arbitrarily shaped underground magazine, we report in

this paper small-scale explosion experiments that test the effect of the difference in the cross-sectional area between the chamber and the passageway of an underground magazine.

## 2. Experimental details

### 2.1 Test explosive

The test explosive was the same one as used in our previous studies, the details of which are discussed in Sugiyama *et al.*<sup>5)</sup> A 0.50 g pressed pellet made of pentaerythritol tetranitrate (PETN, 95 wt.%) and carbon powder (5 wt.%) was used as an explosive charge, and two pellets were glued together to make a 1.00 g charge. An electrical detonator with 0.1 g of lead azide was glued to the top of the pellets. Our data, as well as those from previous papers<sup>5),6),8)</sup>, are expressed in terms of a distance  $K$  ( $\text{m kg}^{-1/3}$ ) scaled to the mass of the explosive, where  $1 \text{ m kg}^{-1/3}$  corresponds to 100 mm in the scale models used below since the released energy from the detonator was estimated as about 2 % of that from the PETN pellets<sup>13)</sup>, and is negligible to calculate the scaled distance.

### 2.2 Setup

The experimental setup was like the setups that we have used in the past<sup>5),6)</sup>. For underground magazines regulated in Article 25 of Japan's Ordinance for Enforcement of the Explosive Control Act, a protective dike must be located near the exit to minimize the damage caused by blast waves and fragments, so we include a dike model in our tests. Figure 1 shows a schematic of the magazine, cover, exit, and dike mounted on a steel plate; the inner diameters of the chamber and the passageway were fixed at 38.8 mm and 19.8 mm, respectively.  $L_0$  and  $L_1$  marked in red in Figure 1 are defined as lengths of the chamber and passageway, respectively, and varied as parameters in the present tests, and Table 1 summarizes the parameters in the present (labeled Case 1 to Case 3)

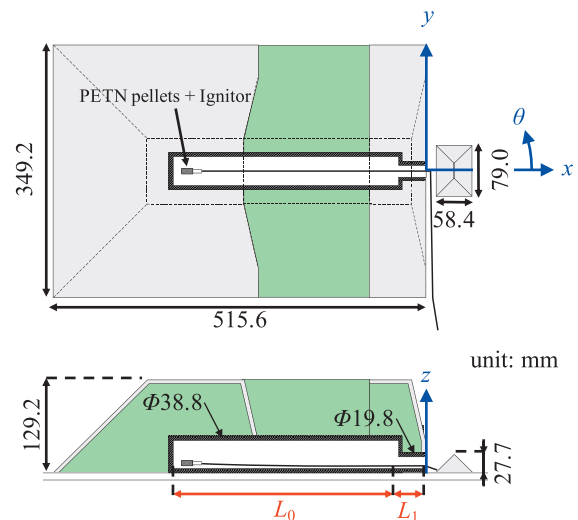


**Figure 1** Schematics of the scale-model magazine and dike.  $L_0$  and  $L_1$  denote lengths of the chamber and passageway, respectively. The lengths marked in red ( $L_0$  and  $L_1$ ) are varied in the three cases tested in the present study, and  $L_0 + L_1 = L = 349.2$  mm.

**Table 1** Parameters in the present (labeled Case 1 to Case 3) and previous (noted as 2017<sup>6)</sup>) tests.

Exp.	$L_0$ [mm]	$L_1$ [mm]	$L_1/L_0$
2017 <sup>6)</sup>	349.2	0	0
Case 1	310.4	38.8	0.125
Case 2	232.8	116.4	0.5
Case 3	116.4	232.8	2.0

and previous (noted as 2017<sup>6)</sup>) tests. Due to the fact that we did not divide the underground magazine into two sections of the chamber and the passageway in the previous study, the conditions in our 2017 experiment<sup>6)</sup> are described as  $L_0 = 349.2$  mm and  $L_1 = 0$  mm ( $L_1/L_0 = 0$ ) in Table 1. The total length  $L = (L_0 + L_1)$  is fixed at 349.2 mm, and therefore we only varied the length ratio,  $L_1/L_0$ , between the chamber and passageway lengths.

The other main difference between the tests discussed in the present article and our previous tests<sup>6)</sup> was the dike size. The size of the dike was designed with reference to the line of sight from outside the magazine opening to the high explosive charge in the chamber. The dike in the present study was made just high enough that its top obscures the line of sight to the charge for the magazine dimensions tested in Case 1. Since the passageway was narrower than the chamber, the dike was almost half the height of the dike in the previously tested scale models<sup>5)-7)</sup>.

The scale-model magazine was constructed from a cylindrical steel pipe with 6 mm thick walls. The height of the scale-model cover was 129.2 mm. Due to the fact that complex blast-wave reflections occur around the exit and dike model, a solid wall near the exit is required to maintain the shape of the exit and ensure the repeatability of the measurements. Therefore, the scale-model exit wall was made of steel, as shown in the exit model in Figure 1. We filled the space between the scale-model exit and the cover with clay of density 2230 kg m<sup>-3</sup>. Since the acoustic impedance of clay is much larger than that of air, any energy absorbed in the clay from the air can be neglected.

The center of the explosive charge was placed 20 mm from the end wall of the magazine model. The origin of the ( $x, y, z$ ) coordinate system is placed at the exit of the magazine model on the steel plate, and the azimuth angle is defined as increasing counterclockwise from the  $+x$ -axis, as shown in Figure 1.

### 2.3 Measurement

The blast-wave pressures were recorded using a digital waveform recorder (H-TECH Triple Mode 30622) and piezoelectric pressure sensors (PCB 113B28, 14.5 mV kPa<sup>-1</sup>). The distances between the magazine exit and the pressure sensors on the base plate were 400, 800, 1200, and 1600 mm; the corresponding distances scaled to the mass of the charge are  $K = 4, 8, 12,$  and  $16$ , respectively. Due to the fact that the magazine model is symmetric with respect to the  $z$ - $x$  plane, the pressure distribution only needs to be measured from azimuth angles  $0^\circ$  to  $180^\circ$ , and sensors were placed to measure pressure in azimuth

intervals of  $10^\circ$  between  $0^\circ$  and  $180^\circ$ . The pressure sensor at  $K = 4$  was covered by the underground magazine model between  $160^\circ$  and  $180^\circ$ , so we did not measure the pressure-time histories at these points.

In addition, we conducted surface-explosion experiments without any scale-model magazine to assess how the magazine structure attenuates an unimpeded blast wave. The explosive was placed vertically to generate a two-dimensional axisymmetric blast wave and the height between its center and the steel plate was 0.18 m kg<sup>-1/3</sup>. A series of explosion tests were conducted in order to confirm the reproducibility of the peak-overpressure distribution and to determine how the azimuth angle affects the blast wave emerging from the exit. The data discussed were values averaged over two or three trials.

### 3. Results and discussion

Figure 2 shows the pressure-time histories at distances in the range  $4 \leq K \leq 16$  along the azimuth angle  $0^\circ$  for the tests conducted in (a) 2017<sup>6)</sup>, (b) Case 1, and (c) Case 3. On the vertical axis (overpressure), one increment in Figures 2(a)–2(c) represents 20 kPa.

As the incident blast wave reached the pressure sensor, the overpressures increased suddenly, and the peak overpressure was recorded. The peak overpressures in 2017 experiments<sup>6)</sup> were higher than those measured in Cases 1 and 3. In Cases 1 and 3, after the peak overpressure, multiple small peaks appeared after the initial blast wave. After the blast wave reaches the junction of the chamber and the passageway, only some of the blast wave propagates directly through the passageway and exits via the opening. The rest of the blast wave reflects off the walls of the junction. The reflected wave propagates back and forth inside the chamber and repeatedly releases some pressure through the junction between the chamber and the passageway. This causes a series of blast waves to exit from the magazine opening, resulting in the series of pressure peaks shown in Figures 2(b) and 2(c). In the case of the 2017 tests<sup>6)</sup>, with no junction inside the underground magazine, only one blast wave exits from the opening, so all the energy from the high explosive charge was released from the exit at once. In the tests reported in this article, only some of the total energy is released each time a blast wave exits the magazine, making the maximum overpressure values measured in Cases 1–3 lower overall than those measured in 2017<sup>6)</sup>.

This division of the blast waves may also affect the positive impulse values. The positive impulse is calculated as the time integral of the positive overpressure readings from the time at which the first incident blast wave is recorded to the time at which the overpressure first returns to zero. As measured at  $K = 16$  in Figures 2(b) and 2(c), the duration between the incident and the second peak was 0.74 ms and 0.39 ms, respectively. With a shorter chamber, the period before the generation of the next blast wave is reduced. The second peak in Case 3 appeared during the positive phase, whereas the second

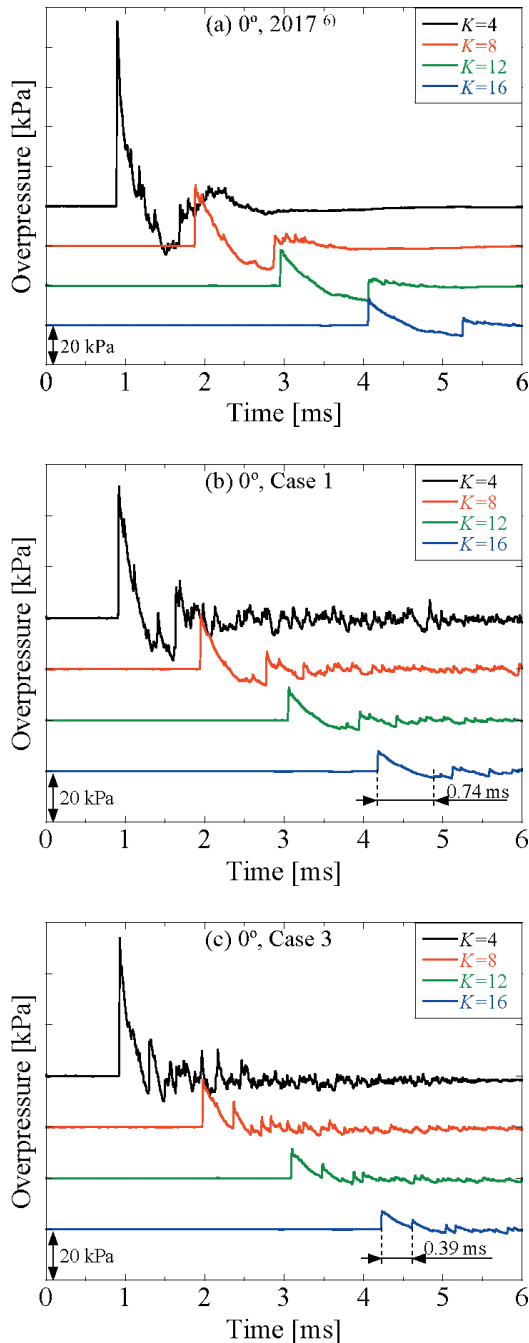


Figure 2 Pressure-time histories.

peak in Case 1 appeared after the positive phase. In Case 3, the second peak lengthened the positive phase and increased the overpressure, which both increased the positive impulse. The second peak at the positive phase in pressure-time histories occurred at several points in Case 3 and increased the positive impulse. Therefore, the length ratio  $L_1/L_0$  seems to affect the positive impulse, and this relationship is discussed further below.

The pressure-time histories were smoothed when calculating the peak overpressures and positive impulses. Figure 3 shows Azimuth angle characteristics of (a, c, e, g) peak overpressure and (b, d, f, h) peak-overpressure ratio. The peak overpressures were normalized with respect to those measured in 2017<sup>6)</sup>. Observation points are  $K = 4$  for (a) and (b),  $K = 8$  for (c) and (d),  $K = 12$  for (e) and (f), and  $K = 16$  for (g) and (h), respectively. Increments of the azimuth angle decreased the peak overpressure, and

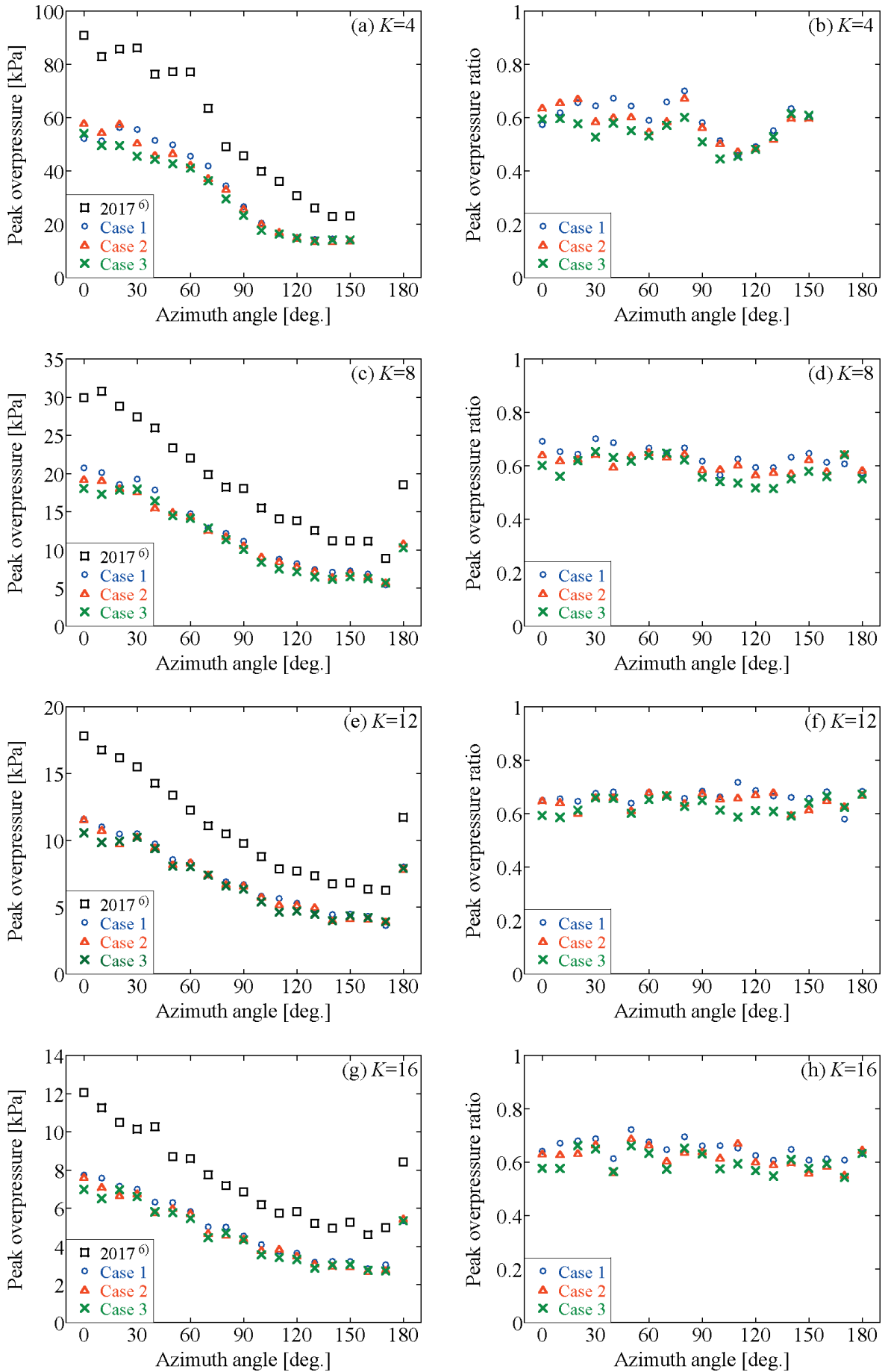
around  $180^\circ$ , the peak overpressure increases locally. Due to the fact that the cover model is symmetrical and has an angular shape as shown in Figure 1, the blast waves propagating behind the cover model are strengthened as they couple together<sup>5)-8)</sup>.

In the present study, as shown in Figure 3, the relatively narrow passageway mitigated the peak overpressures relative to the straight-tube magazine, but the effect was independent of  $L_1/L_0$ . The normalized peak overpressures at  $K = 4$  were distributed azimuthally, and the local minimum value was measured around  $100^\circ$ , as shown in Figure 3(b). This difference is explained by the smaller dike used in the present tests, which alters the reflection and diffraction of the blast wave at the dike. Following the initial development of the blast wave outside the magazine exit, the normalized peak overpressures at  $K = 8, 12,$  and  $16$  were constant at about 0.60 and independent of the azimuth angle.

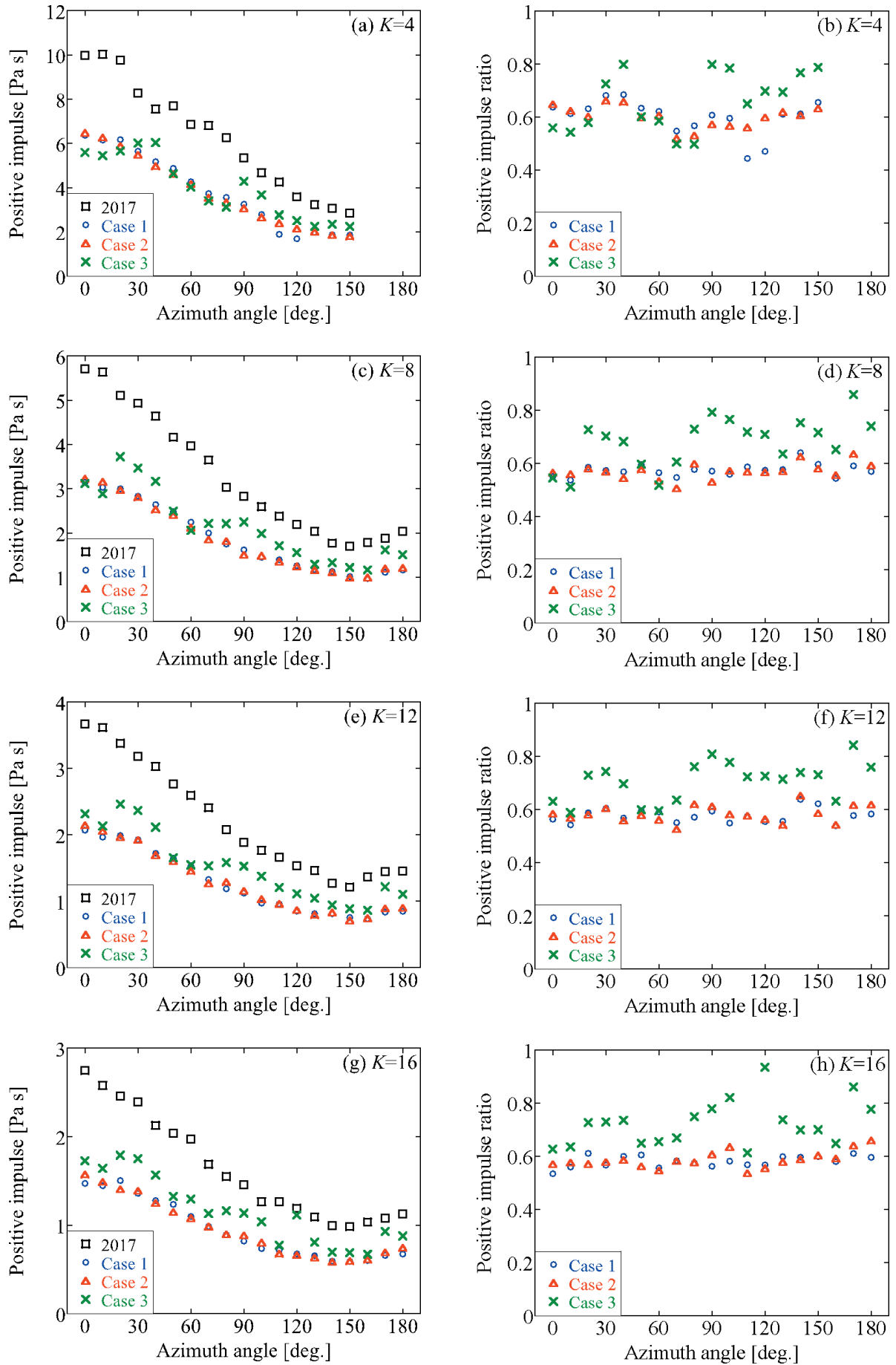
In previous studies, we proposed an empirical equation to model the effects of blast-wave expansion, coupling behind the cover model, and reflection and diffraction off the dike when calculating peak-overpressure distributions, and we leave the detailed discussion of the equation to Refs. 5 and 6. The equation assumes that the peak overpressure at  $0^\circ$  is the primary parameter. The peak-overpressure values calculated with this equation agree well with experimental data taken from fully developed blast waves outside the magazine<sup>5),6)</sup>. Since the normalized peak overpressures at  $K = 8, 12,$  and  $16$  are independent of the azimuth angle, the empirical equation can also estimate the azimuth angle characteristics only by changing the peak overpressure at  $0^\circ$  in the case of the underground magazine with two sections of the chamber and the passageway used in the present study.

Figure 4 shows azimuth angle characteristics of (a, c, e, g) positive impulse and (b, d, f, h) positive impulse ratio. The positive impulses were normalized with respect to those measured (but not published) in 2017. Observation points are  $K = 4$  for (a) and (b),  $K = 8$  for (c) and (d),  $K = 12$  for (e) and (f), and  $K = 16$  for (g) and (h), respectively. The normalized positive impulses are constant at about 0.60 in Cases 1 and 2, as are the normalized peak overpressures. The mitigation of peak overpressure explains the mitigation of the positive impulse in Cases 1 and 2. As denoted above, the second peak at the positive phase in pressure-time histories increased the positive impulse for several points in Case 3 over those in Cases 1 and 2, as shown in Figure 4. However, the positive impulse in Case 3 was always smaller than that in the 2017 tests<sup>6)</sup>, so the length ratio  $L_1/L_0 = 2.0$  had some effect on the mitigation of the positive impulse in the present study. This indicates that some critical value of  $L_1/L_0$  can be found, at which the second peak always appears after the positive phase of overpressure, which would optimally mitigate the positive impulse.

The peak-overpressure distribution is the most important indicator in estimating the ESQD. Therefore, in order to calculate the peak-overpressure distribution, the correlations between the peak overpressure and the



**Figure 3** Azimuth angle characteristics of (a, c, e, g) peak overpressure and (b, d, f, h) peak-overpressure ratio. Observation points are  $K = 4$  for (a) and (b),  $K = 8$  for (c) and (d),  $K = 12$  for (e) and (f), and  $K = 16$  for (g) and (h), respectively. The peak overpressures are normalized with respect to those measured in 2017<sup>6)</sup>.



**Figure 4** Azimuth angle characteristics of (a, c, e, g) positive impulse and (b, d, f, h) positive impulse ratio. Observation points are  $K = 4$  for (a) and (b),  $K = 8$  for (c) and (d),  $K = 12$  for (e) and (f), and  $K = 16$  for (g) and (h), respectively. The positive impulses are normalized with respect to those measured (but not published) in 2017.

**Table 2** Fitting parameters for Equation (2).

$\theta$ [deg.]	Case 1		Case 2		Case 3		2017 <sup>(6)</sup>	
	$l$	$m$	$l$	$m$	$l$	$m$	$l$	$m$
0	-1.377	2.552	-1.455	2.628	-1.473	2.610	-1.456	2.821
10	-1.390	2.551	-1.470	2.620	-1.464	2.572	-1.445	2.790
20	-1.495	2.641	-1.567	2.693	-1.427	2.549	-1.512	2.839
30	-1.501	2.646	-1.447	2.569	-1.386	2.499	-1.542	2.854
40	-1.514	2.622	-1.475	2.546	-1.452	2.526	-1.465	2.754
50	-1.510	2.581	-1.502	2.557	-1.460	2.498	-1.572	2.820
60	-1.494	2.544	-1.447	2.487	-1.460	2.485	-1.597	2.827
70	-1.534	2.529	-1.481	2.458	-1.496	2.465	-1.529	2.707
80	-1.408	2.375	-1.431	2.377	-1.338	2.272	-1.391	2.526
90	-1.273	2.195	-1.268	2.177	-1.205	2.095	-1.383	2.496
100	-1.154	2.003	-1.186	2.026	-1.141	1.947	-1.354	2.415
110	-0.917	1.722	-1.083	1.894	-1.142	1.906	-1.342	2.362
120	-0.859	1.637	-1.026	1.805	-1.073	1.822	-1.222	2.229
130	-1.069	1.819	-1.033	1.775	-1.107	1.814	-1.168	2.132
140	-1.092	1.828	-1.112	1.810	-1.120	1.818	-1.115	2.040
150	-1.060	1.796	-1.119	1.831	-1.095	1.809	-1.085	2.021
160	-1.263	1.984	-1.250	1.948	-1.172	1.866	-1.280	2.198
170	-0.846	1.492	-1.048	1.713	-1.063	1.724	-0.837	1.705
180	-0.978	1.925	-0.980	1.931	-0.923	1.860	-1.139	2.298

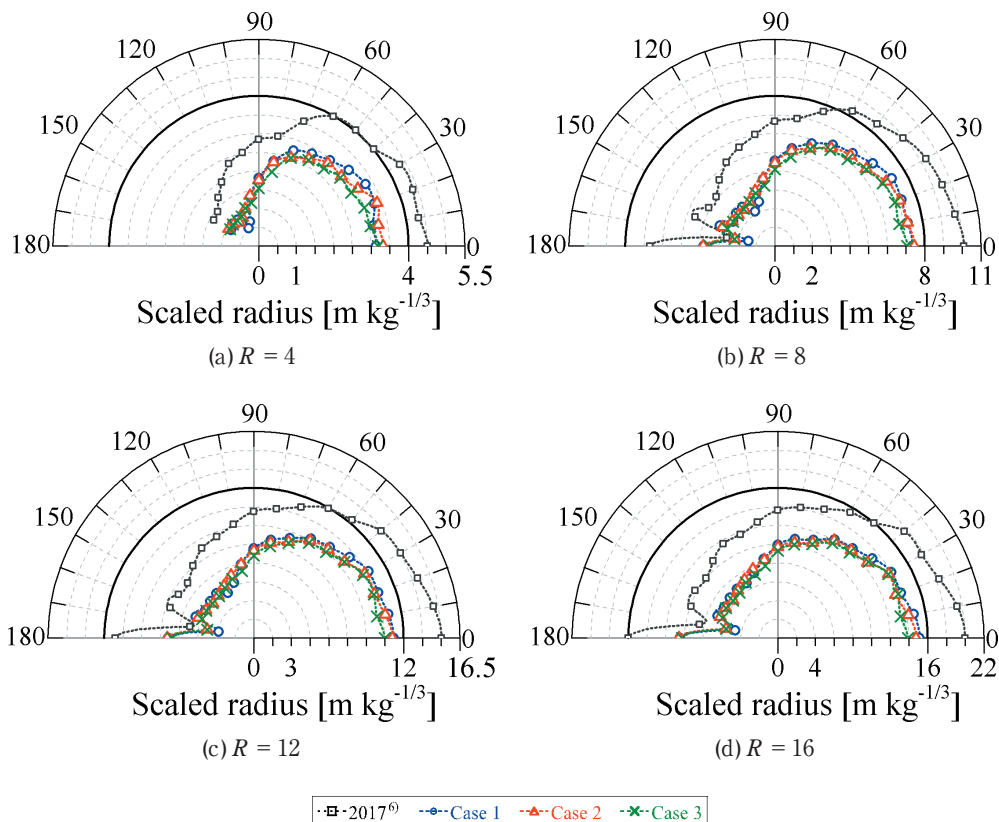


**Figure 5** Isobars of peak overpressure in cylindrical coordinates of scaled radius and azimuth angle. The scaled radius is expressed in terms of a radius from the exit,  $R$  ( $\text{m kg}^{-1/3}$ ), scaled to the mass of the explosive. The peak overpressures correspond to those of the surface-explosion experiments at the scaled radii of (a)  $R = 4$ , (b)  $R = 8$ , (c)  $R = 12$ , and (d)  $R = 16$ . Black solid lines denote the isobars of the surface-explosion experiments.

scaled distance for each experimental condition were fitted with log–log plots. The fitting parameters  $m$  and  $n$  in the following equations are obtained:

$$X = \log K \quad (1)$$

$$\log(p_{\text{peak}}) = lX + m \quad (2)$$

Table 2 lists the fitting parameters obtained from the tests reported in this article.

Figure 5 shows isobars of peak overpressure plotted in cylindrical coordinates and scaled to the radius and azimuth angle obtained from Equation (2). Black solid lines denote the isobars of the surface-explosion experiments because the surface explosion is axisymmetric along  $z$ -axis, and its isobar is described as a circle. The peak overpressures plotted in Figure 5 were measured in surface-explosion experiments at the scaled radii of (a)  $R = 4$ , (b)  $R = 8$ , (c)  $R = 12$ , and (d)  $R = 16$ . Here, the scaled radius is expressed in terms of a radius from the exit,  $R$  ( $\text{m kg}^{-1/3}$ ), scaled to the mass of the explosive. The origin coincides with the point from which the blast wave expands, which is the exit in the underground magazine model tests and the charge location in the surface-explosion experiments. Narrower passageways greatly reduced the size of the isobars in Cases 1–3, and they were always smaller than those of the surface-explosion experiments. Since the shape of isobars were independent of  $L_1/L_0$ ,  $L_1/L_0$  would not need to be considered when calculating the ESQD from the peak-overpressure distribution. Previous studies<sup>2),3),13)</sup> indicated that the peak overpressure of the shock wave at the magazine exit and the size of the exit determine the strength of the blast wave outside. Since the ratio between the diameters of the chamber and the passageway is fixed to 0.51 in the present study, the peak overpressures measured in Cases 1–3 would be similar. Further testing is needed to reveal the effect of the diameter ratio on the strength of the blast wave outside the magazine exit.

#### 4. Conclusion

We conducted scale-model explosion experiments in order to determine how the presence of a narrow passageway to a chamber affects the azimuthal distribution of a blast wave exiting an underground magazine. In this study, a scale-model underground magazine was divided into a chamber and a passageway, so that the length ratio,  $L_1/L_0$ , between the chamber ( $L_0$ ) and the passageway ( $L_1$ ) could be varied. The experiments showed that a relatively narrow passageway greatly mitigates the strength of the blast wave, but the ratio of

the passageway to the chamber lengths did not influence the peak overpressure and isobars outside the exit.  $L_1/L_0$ , therefore, would not need to be measured to determine the ESQD from isobars of peak overpressure. Small length ratio  $L_1/L_0$  changed the observation time of the second peak after the initial blast wave. When it appeared at the positive phase, the positive impulse increased. Then, some critical value of  $L_1/L_0$  could be found, at which the second peak appears after the positive phase, which would optimally mitigate the positive impulse.

#### Acknowledgment

This study was made possible by a Ministry of Economy, Trade, and Industry (METI) sponsored project entitled “Technical Standard for Explosion Mitigation of Explosives” in FY2017.

#### References

- 1) M. S. Mannan, “Lees’ Loss Prevention in the Process Industries, 4th Edition: Hazard Identification, Assessment and Control”, Butterworth-Heinemann (2012).
- 2) C. N. Kingery and E. J. Gion, BRL-TR-3132, Ballistics Research Laboratory (1990).
- 3) Y. Sugiyama, K. Wakabayashi, T. Matsumura, and Y. Nakayama, *Sci. Tech. Energetic Materials*, 76, 14–19 (2015).
- 4) A. T. Skjeltop, R. Jossen, and A. Rinnan, *Proc. Fifth International Symposium on Military Application of Blast Simulators*, p. 6:7:1, Stockholm, (1977).
- 5) Y. Sugiyama, K. Wakabayashi, T. Matsumura, and Y. Nakayama, *Sci. Tech. Energetic Materials*, 77, 136–141 (2016).
- 6) Y. Sugiyama, K. Wakabayashi, T. Matsumura, and Y. Nakayama, *Sci. Tech. Energetic Materials*, 78, 117–123 (2017).
- 7) Y. Sugiyama, K. Wakabayashi, T. Matsumura, and Y. Nakayama, *Sci. Tech. Energetic Materials*, 78, 49–54 (2017).
- 8) Y. Sugiyama, K. Wakabayashi, T. Matsumura, and Y. Nakayama, *Sci. Tech. Energetic Materials*, 79, 28–33 (2018).
- 9) Y. Nakayama, T. Matsumura, M. Iida, and M. Yoshida, *Kayaku Gakkaishi (Sci. Tech. Energetic Materials)*, 62, 244–255 (2001). (in Japanese).
- 10) Y. Nakayama, D. Kim, K. Ishikawa, K. Wakabayashi, T. Matsumura, and M. Iida, *Sci. Tech. Energetic Materials*, 69, 123–128 (2008).
- 11) D. Kim and Y. Nakayama, *Sci. Tech. Energetic Materials*, 71, 88–91 (2010).
- 12) C. N. Kingery, Technical Report BRL-TR-3012, June (1989).
- 13) M.A. Price and A.H. Ghee, *Cent. Eur. J. Energetic Materials*, 6, 239–254 (2009).